Exergoeconomic assessment of green hydrogen production via high-temperature electrolysis powered by solar and wind energy

Diego Luis Izidoro[a,b], Silvio de Oliveira Junior[c]

[a] Instituto Federal de Educação Ciência e Tecnologia de Minas Gerais - Campus Formiga, Formiga - MG, Brasil, diego.izidoro@ifmg.edu.br
[b] Escola Politécnica, Universidade de São Paulo, São Paulo - SP, Brasil, diego.izidoro@usp.br
[c] Escola Politécnica, Universidade de São Paulo, São Paulo - SP, Brasil, soj@usp.br

Abstract:
Hydrogen is considered a promising alternative as an energy carrier for the transition to a renewable energy matrix. However, most of the hydrogen is currently produced using fossil fuels, making it essential to develop green hydrogen production routes. Therefore, this study aims to perform an exergoeconomic analysis of the high-temperature electrolysis (HTE) process for hydrogen production using solar and wind energy. To this end, it is proposed novel plant arrangements for solid oxide electrolysis cells (SOEC). To supply the plant's electrical demand, two options are considered: a wind farm (WF) and a photovoltaic system (PV). A solar concentration system is considered for the thermal demand. As another contribution to the area, the analysis is carried out considering the Brazilian scenario, specifically Pecém (Ceará), a coastal district located in the northeast of Brazil. It was selected due to the high availability of solar and wind resources and the existing industrial and port infrastructure. Energy and exergy analyses are performed to identify the components with the highest level of irreversibility. Finally, an exergoeconomic assessment is accomplished to determine the exergy costs of hydrogen production. For the WF-SOEC arrangement, the total exergy efficiency obtained is 26.53%, and the unit exergy cost of hydrogen is 3.89 kJ/kJ. For the PV-SOEC arrangement, the corresponding values are 13.74% and 7.53 kJ/kJ, respectively. Overall, the results demonstrate that HTE route using solar and wind energy can be a viable and sustainable alternative to produce hydrogen from 100% renewable sources and without direct CO_2 emissions.

Keywords:
Exergoeconomic assessment; Green hydrogen; Solar energy; Wind energy.

1. Introduction

Hydrogen plays an important role in the chemical industry. Industrial hydrogen is utilized for various purposes such as producing fertilizers and ammonia, refining petrochemicals, processing food, cooling power generators in power plants, metallurgical processes, as a fuel for space exploration, and manufacturing semiconductors [1][2].

In addition to being an important industrial raw material, hydrogen has the potential to become a key energy source for achieving sustainable decarbonization, particularly in sectors where electrification is difficult [3][4] From a total cost perspective (including production, distribution and retail costs), hydrogen could be the most cost-effective low-carbon solution for more than twenty different applications, including long-distance transportation by road and sea, urban vehicles, trains, the steel industry, energy storage, and residential heating [5][6].

Hydrogen can be produced using different non-renewable (coal, oil, nuclear and natural gas) or renewable (biomass, solar, wind, hydro, geothermal, wave energy, etc.) resources through a wide variety of technological routes (reforming, gasification, electrolysis, etc.) [7]. To be considered low-carbon hydrogen, it must be produced from renewable electricity, nuclear, biomass or fossil fuels with carbon capture, storage and utilization (CCUS). However, almost all the hydrogen is currently generated from fossil fuels without CCUS [8].

Electrolysis is one of the oldest and most mature processes and has the versatility to use electricity from different renewable sources to produce H_2. Alkaline electrolysis stands out for being the one with the greatest maturity and the greatest commercial reach [9]. PEM (polymer electrolyte membrane) electrolysis have many advantages such as lower gas permeability, high proton conductivity, and high pressure operation [10]. However, as the temperature rises, the electrolysis process becomes more endothermic and a greater proportion of the total energy needed for the system can be provided in the form of heat, leading to increased efficiency in the process [11].

https://doi.org/10.52202/069564-0018

In this way, high-temperature electrolysis (HTE) offers higher efficiency by operating at reduced electrical potentials, thereby minimizing irreversibilities. The high operating temperature is an important feature of this process, giving rise to its two main advantages over alkaline and polymeric membrane electrolyzers: higher exergy efficiencies and faster chemical kinetics [12]. Despite being a process under development, it is approaching maturity. HTE occurs through solid oxide electrolyzer cells (SOEC) operating in the range of 600°C to 900°C. SOECs can convert steam (H_2O), carbon dioxide (CO_2), or a combination of both, directly into hydrogen (H_2) or syngas (H_2+CO), respectively. HTE can be integrated with various renewable energy sources and industrial processes. These can serve as feedstocks for fuel synthesis plants and the chemical industry, thus enabling different Power-to-X scenarios. They can also be integrated with various chemical synthesis processes for the recycling of captured CO_2 and H_2O into synthetic fuels such as methane, methanol, and ammonia. When operating in reverse, the electrolyzer cell acts as a solid oxide fuel cell (SOFC) [13].

Some authors [14][15][16][17][18][19] have previously proposed plant layouts for solid oxide electrolyzer cells that operate from renewable sources, specially solar energy. However, these studies have mainly focused on technical and economic analysis, with an emphasis on energy and capital costs. In general, energy balances treat all energy forms as equal without distinguishing between different degrees of energy that pass through the system boundary and do not provide information on internal losses. Exergy analysis, which is an alternative technique based on the concept of exergy, can be used to address this limitation [20][21]. And from the perspective of modeling, simulating, and optimizing energy systems, exergoeconomic assessment is also important in determining the average cost per unit of exergy of each exergy stream [22].

Based on this background, the present study makes a significant contribution to the area by employing a comprehensive evaluation methodology based on energy, exergy, and exergoeconomic assesment for two novel plant arrangements for H_2 production based on the HTE route, powered by solar and wind energy. This assessment provides a comprehensive thermodynamic evaluation of the plant processes. In addition, the study focuses on the Brazilian scenario, specifically Pecém (Ceará), which is a location in northeastern Brazil with high availability of solar and wind resources and existing industrial and port infrastructure - optimal conditions for a hydrogen production plant.

2. Method

2.1. SOEC modelling

The process of electrolyzing water to produce hydrogen and oxygen gases is a long-standing and established method. The basic principle of an electrolyzer is to use electricity to split water molecules. This phenomenon was initially demonstrated by Nicholson and Carlisle in 1800, and further expounded upon by Faraday in the 1820s, who coined the term "electrolysis" in 1834. However, it was only in 1902 that the Oerlikon Engineering Company began the commercial use of electrolysis [11]. The reaction for water electrolysis can be represented by the Eq. (1):

$$H_2O \rightarrow H_2 + 1/2\, O_2 \tag{1}$$

Solid oxide electrolyzer models can be classified into several types. Geometrically, they are categorized into zero-dimensional (0D), one-dimensional (1D), two-dimensional (2D), and three-dimensional (3D) models. They can also be classified as physical models (white-box), empirical models (black-box), and semi-empirical models (gray-box). Additionally, in terms of length scale, SOEC models can be classified into microscale, mesoscale, and macroscale models, with the latter further subdivided into cell-level, stack-level, and system-level models [23]. In this study, a semi-empirical SOEC (zero dimension) system model was developed according to the studies of O'Brien [12], Petipas, Brisse and Bouallou [24], and Hansen [25].

The minimum electrical energy (W_{min}) required for electrolysis (reversible process) is equal to the change in Gibbs free energy (G), shown in Eq. (2), where H represents the enthalpy, T is the absolute temperature and S the entropy of the reactants and products of the chemical reaction. With increasing temperature, the electrolysis process becomes progressively endothermic.

$$\dot{W}_{min} = \Delta G = G_{prod} - G_{react} = H_{prod} - H_{react} - T(S_{prod} - S_{react}) \tag{2}$$

For the electrolysis process to take place, the minimum voltage required is the standard state open-cell voltage or reversible voltage (V_0) given by Eq. (3), where ΔG is the Gibbs free energy change, F is the Faraday constant (96,486 C/mol) and j is the number of electrons transferred per molecule of hydrogen produced.

$$V_0 = \frac{\Delta G}{jF} \tag{3}$$

When reactants and pure products are separated, the reversible voltage (V_0) is applicable [26]. However, to account for the variety of gas compositions present in real electrolyzers, the Nerst open cell potential (V_N) must

be considered, as given by Eq. (4), where R_u is the universal gas constant, y represents the molar fractions and T is the absolute temperature during the reaction.

$$V_N = \frac{\Delta G}{jF} - \frac{R_u T}{jF} ln\left(\frac{y_{H_2O}}{y_{H_2} y_{O_2}^{0,5}}\right) \quad (4)$$

The thermoneutral voltage (V_{TN}), as a function of the enthalpy of reaction (ΔH), is given by Eq. (5). The electrolysis of water is an endothermic process. Therefore, the heat flux of the reaction ($q"_R$) is negative. However, the heat flux resulting from irreversibilities ($q"_{OHM}$), is positive. At thermoneutral voltage, the net heat flux is zero, as these heat fluxes cancel each other out [26]. Their values can be calculated using Eq. (6) where i is the current density (A/m²).

$$V_{TN} = \frac{\Delta H}{jF} \quad (5)$$

$$q"_R = -q"_{OHM} = i(V_N - V_{TN}) \quad (6)$$

The electrical power ($\dot{W}_{TN}$) required for the electrolysis process considering the thermoneutral voltage can be calculated using Eq. (7), where I is the current (A) in the electrolyzer and $\dot{m}_{H_2}$ is the mass flow rate of hydrogen.

$$\dot{W}_{TN} = V_{TN} I = \dot{m}_{H_2} \Delta H \quad (7)$$

The modelling and simulation of the electrolysis process is performed via Python using the suite Cantera [27] and the Coolprop library [28].

2.2. Proposed plants

An electrolysis plant is basically composed of electrolyzers and the Balance of Plant (BoP), which includes energy supply, water supply and purification, compression, processing, and storage of gases. Figure 1 illustrates two hydrogen production plants. The first involves a wind farm supplying electricity to solid oxide electrolysis cells (WF-SOEC), proposed initially in a previous study [29]. In the second plant, photovoltaic panels (PV-SOEC) supply all the electrical energy needed. In both cases, to provide the necessary thermal energy, a solar tower system is used, whereby solar radiation is collected by heliostats in the solar field and reflected to superheat steam at a temperature of 850°C in the solar receiver (SR).

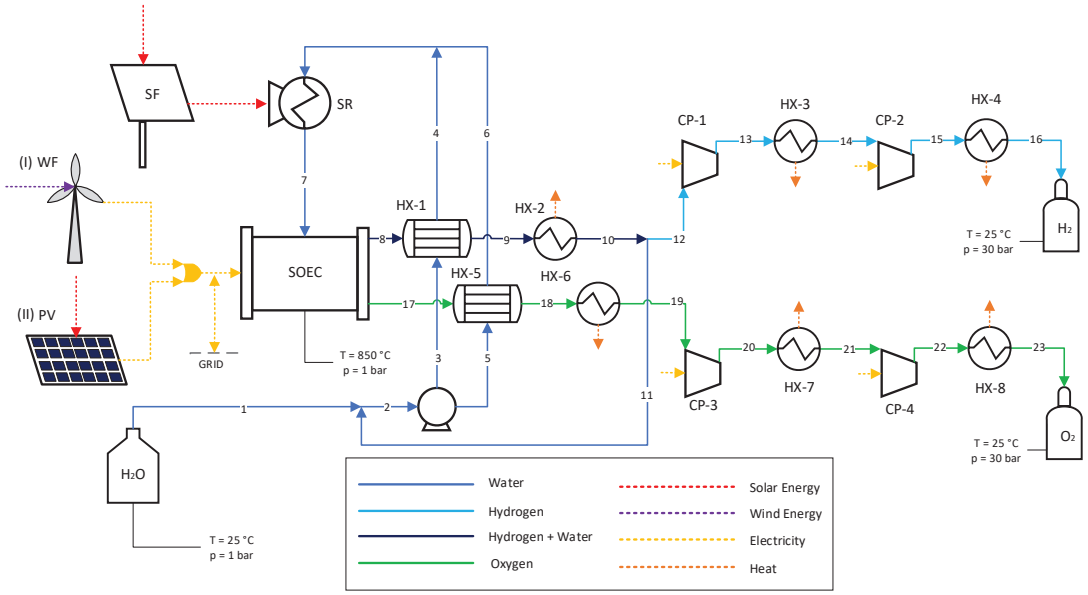

Figure 1. Proposed plants: (I) WF-SOEC (II) PV-SOEC

The electrolyzer produces two streams, one containing a mixture of hydrogen (H_2) and steam, and the other containing oxygen (O_2), which are then directed to recovery heat exchangers (HX-1 and HX-5, respectively) to preheat the water used in the process. The H_2/H_2O mixture is then cooled in HX-2, and the condensed steam is separated from hydrogen and recycled. Finally, hydrogen and oxygen are compressed (H_2 in CP-1 and CP-2, and O_2 in CP-3 and CP-4) and cooled (H_2 in HX-3 and HX-4, and O_2 in HX-6, HX-7, and HX-8)

https://doi.org/10.52202/069564-0018

before being stored at a pressure of 30 bars. The main differences in relation to other arrangements proposed in the literature are related to the direct recovery of heat from the electrolyzer outlet gases and the processing and storage of oxygen as a co-product.

The wind farm (or photovoltaic panels) also provides the necessary electricity to power the compressors, but due to the intermittent nature of electricity production, a connection to the electrical grid is also included. For the analysis of the proposed systems, the following conditions are considered:

- The hydrogen production plant is designed to operate for eight hours a day according to the supply of concentrated solar energy [30].
- In the WF-SOEC arrangement, the installed capacity of the wind farm is 10 MW (five Vestas V100-2MW wind turbines) [31].
- In the PV-SOEC arrangement, the installed capacity is considered the minimum necessary to produce the equivalent amount of H_2 in the WF-SOEC arrangement.
- The efficiency of PV system, defined as the ratio between the output electricity and the input of solar energy, is 15%.
- The AC-DC electricity conversion efficiency is 95%.
- The solar field (SF) has an energy efficiency of 60% [17], which means that only 60% of the solar energy reaching the heliostats is directed to the receiver (the remaining 40% are heat and optical losses).
- The solar receiver (SR) has an energy efficiency of 85% [32], which is the percentage of energy absorbed by the steam in the component (the remaining 15% are heat and optical losses).
- The electrolyzer operates at a thermoneutral voltage to minimize thermal stress [12]. Consequently, the process is isothermal at T = 850ºC and p = 1 bar.
- The molar steam conversion ratio (SC) is 75%, i. e., the molar fraction of H_2 at the SOEC outlet is 0.75 [24].
- Each compressor has an isentropic efficiency of 80%.
- Heat recovery exchangers HX-1 and HX-5 do not transfer heat to the environment, and pinch point is 10°C. The thermodynamic state of the water is the same at the outlet of these both heat exchangers.
- Pressure losses, as well as changes in kinetic and potential energy are not considered.

3.3. Solar and wind data

The study is being carried out for Pecém, a coastal district located in north-eastern Brazil. This location was selected due to its established industrial, electrical, and port infrastructure, as well as its abundance of solar and wind energy resources. Furthermore, there is a project to establish a green hydrogen hub in the area [33].

Data for solar resource evaluation are taken from The National Solar Radiation Data Base (NRSDB) through System Advisor Model (SAM) software considering a typical meteorological year (TMY) [34][35]. The average daily global horizontal irradiation (GHI) is estimated at 6.19 kWh/m²/day and the average daily direct normal irradiation (DNI) is estimated at 5.95 kWh/m²/day.

For the wind resource evaluation, it was used the data from the atlas of Brazilian wind potential [36]. The wind speed distribution can be represented by the Weibull density probability function, given by Eq. (8), where v is the wind speed, c is the scale factor and k is the form factor [37]. The main wind parameters for Pecém considering a height of 100 meters are presented in Tab. 1.

$$f(v) = \frac{K}{C}\left(\frac{v}{C}\right)^{K-1} e^{-(v/C)^K} \tag{8}$$

The monthly mean values of direct normal irradiance (DNI) and global horizontal irradiance (GHI) for Pecém in a TMY are shown in Figure 2a. The annual wind speed distribution is shown in Figure 2b, considering the number of annual hours for different speed intervals.

Table 1. Main wind parameters

Parameter	Unit	Value
Average wind speed ($\bar{v}$)	m/s	8.87
Scale factor (C)	-	9.76
Form factor (K)	m/s	4.20
Average air density (ρ)	kg/m³	1.17

Source: [36]

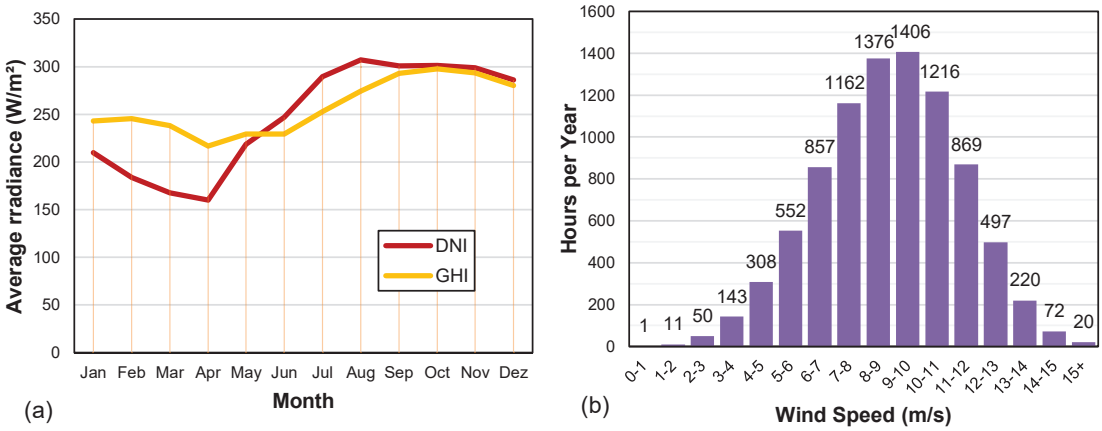

Figure 2. Solar and wind data for Pecém: (a) Solar irradiance [34][35] *and (b) Wind speed distribution* [36].

3.4. Energy and exergy analysis

The efficiency of energy conversion in SOEC system (η_{SOEC}) can be defined analogously to the definition for fuel cells in terms of the enthalpy of reaction according to Eq. (9) and the solar/wind-to-hydrogen conversion efficiency can be calculated in terms of the higher heating value of hydrogen (HHV) with Eq. (9):

$$\eta_{SOEC} = \frac{\dot{m}_{H_2} \Delta H}{\dot{W}_{SOEC}} \tag{9}$$

$$\eta_{solar/wind\_H_2} = \frac{\dot{m}_{H_2} HHV_{H_2}}{\dot{W}_{WF/PV} + \dot{Q}_{SF}} \tag{10}$$

The exergy efficiency of the electrolysis process can be defined according to the expression of Eq. (11), called the degree of perfection, being the ratio between the exergy of the products and the input exergy:

$$\eta_{B,SOEC} = \frac{B_{prod}}{B_{input}} = \frac{\dot{B}_8 + \dot{B}_{17}}{\dot{B}_7 + \dot{W}_{SOEC}} \tag{11}$$

The wind turbine exergy ($\dot{B}_{WF,in}$) is expressed by Eq. (12), which is a function of the air specific mass (ρ), the turbine swept area (A), and the wind speed (v) [38]. For the exergy analysis of solar field (SF) and photovoltaic panels (PV), the relation between energy and exergy fluxes in Eq. (13) is considered [39], where T is the solar surface temperature (5778 K) and T_0 is the ambient temperature (298 K). For these specific values, the ratio between exergy and energy fluxes is 0.9312.

$$\dot{B}_{WF,in} = \frac{1}{2}\rho A v^3 \tag{12}$$

$$\frac{\dot{B}_{SF/PV,in}}{\dot{E}_{SF/PV,in}} = 1 - \frac{4}{3}\frac{T_o}{T} + \frac{1}{3}\left(\frac{T_0}{T}\right)^4 \tag{13}$$

The exergy efficiencies for the solar field (SF), solar receiver (SR), wind farm (WF), photovoltaic panels, electrolyzer (SOEC), and heat exchangers HX-1 e HX-5 are defined as the ratio between output and input exergy. As for the compressors, their exergy efficiencies were determined by the ratio of the exergy change and the power provided. The total exergy efficiency of the plant was calculated as a function of the total fluids exergy rates and the solar radiation exergy rates with Eq. (14):

https://doi.org/10.52202/069564-0018

$$\eta_{B,total} = \frac{\dot{B}_{H_2.16} + \dot{B}_{O_2.23}}{\dot{B}_{WF/PV,in} + \dot{B}_{SF,in} + \dot{B}_{water.1}} \quad (14)$$

3.5. Exergoeconomic assessment

Based on Fig. 3, the exergoeconomic balance can be written according to Eq. (15), where $\dot{C}_{inp,i}$ and $\dot{C}_{prod,i}$ are the cost rates of inputs and products, respectively.

Figure 3. Exergoeconomic balance components

$$\sum_i \dot{C}_{inp,i} = \sum_i \dot{C}_{prod,i} \quad (15)$$

Eq. (15) can be rewritten, inserting the unit exergy cost, c_i, (in kJ/kJ) for each stream, according to Eqs. (16) and (17). It represents the amount of exergy required to produce a unit of the respective exergy stream. In this way, it is considered that the input used in the first process of a plant has an exergy cost equal to the unit.

$$c_i = \frac{\dot{C}_i}{\dot{B}_i} \quad (16)$$

$$\sum_i (c_{inp} \cdot \dot{B}_{inp})_i = \sum_i (c_{prod} \cdot \dot{B}_{prod})_i \quad (17)$$

When necessary, partition methods are applied, as proposed by [40]: Equality method: the costs are divided among the products according to their exergy content; (ii) Extraction method: the costs are discharged in a single exergy stream.

The product of multiplying the unit exergy cost (kJ/kJ) by the specific exergy of a given stream (kJ/kg) produces an exergy intensity indicator in kJ/kg that specifies the amount of exergy required to obtain a unit of mass of a certain stream [41], according to Eq. (18):

$$\varphi_i = c_i b_i \quad (18)$$

4. Results and Discussion

Figure 4a illustrates the wind exergy and generated electricity for the analysed wind farm as function of wind speed. Figure 4b shows the corresponding exergy efficiencies. The maximum net power output of 10 MW is achieved only when wind speed exceeds 11.6 m/s, which happens 12.7% of the time, or approximately 1110 hours per year. The average net power output is estimated as 6.38 MW. The total yearly electricity generation in the wind farm is estimated as 55.88 GWh. Considering a total of 170.5 GWh of wind exergy available annually, this represents an average exergy efficiency of 32.8%.

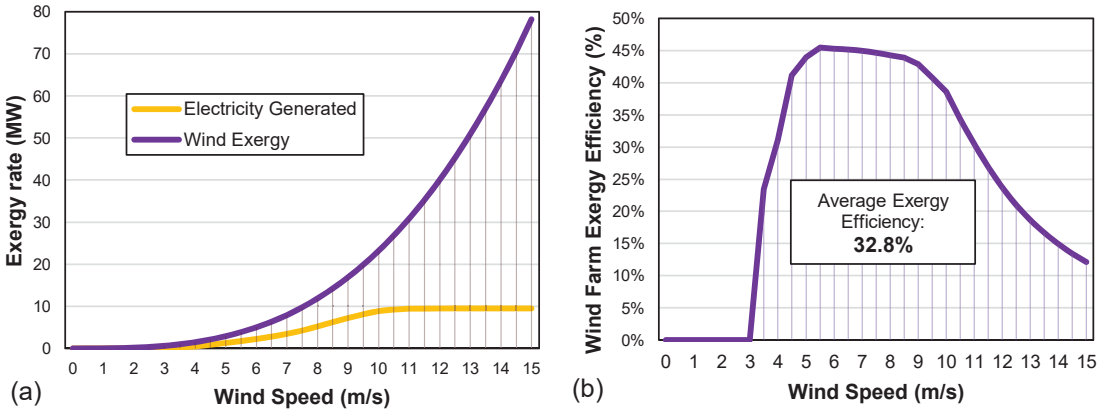

Figure 4. Wind farm results: (a) Wind exergy and electricity generated and (b) Exergy efficiency

The estimated electricity generation over a typical meteorological year (TMY) is shown in Fig. 5 in GWh for the two considered systems (WF and PV). The months with the highest and lowest levels of generation coincide for both forms of generation. However, the variability of wind energy is slightly higher. Fig. 6 illustrates the hydrogen production of the proposed plant. The estimated average daily production of hydrogen is 4.13 t, which results in a daily production of 23.7 t of oxygen and a water consumption of 36.8 m³/day. Due to the variation in direct irradiation throughout the year, the production in April tends to be 48% lower than in August. In practice, it means that the plant would operate at about half of its capacity during this month.

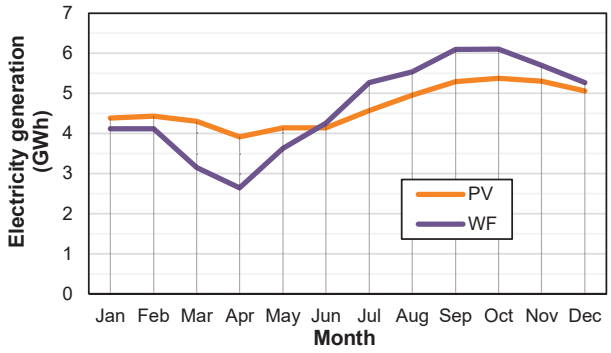

Figure 5. Estimated electricity generation over a typical meteorological year (TMY)

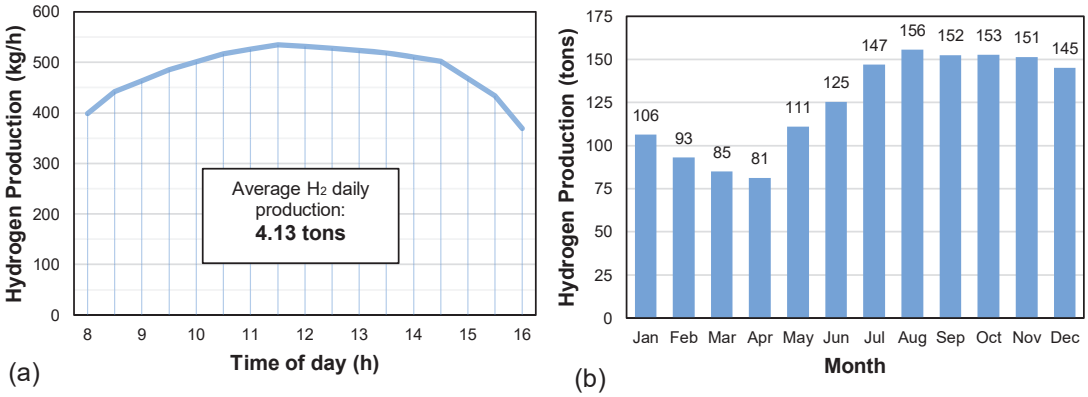

Figure 6. Hydrogen production: (a) Average hourly production and (b) Average production per month

Table 2 summarizes the results of the energy and exergy analysis conducted for the plant's power and heat supply components. The irreversibilities observed in wind turbines are associated with the interaction between air and blades, as well as the efficiencies of mechanical and electrical conversion. In the PV panels and solar concentrators there are optical losses such as attenuation, blocking, or shadowing, as well as losses related to heat convection and conduction [39]. For the wind farm, the values from the energy and exergy analysis are the same since wind exergy and electrical work are equal to the values in the exergy balance. For the PV panel, solar field and solar receiver, the ratio between exergy and input energy is given by Eq. (13). Specifically for the solar receiver, the exergy efficiency is much lower than the energy efficiency due to the irreversibility of the process of converting solar radiation into exergy of the steam.

Table 2. Energy and exergy analysis: power supply components

Components[1]	Energy Analysis			Exergy Analysis		
	Received (MWh/day)	Delivered (MWh/day)	Energy Efficiency (%)	Received (MWh/day)	Delivered (MWh/day)	Exergy Efficiency (%)
Wind Farm (WF)	467.19	153.09	32.8	467.19	153.09	32.8
Photovoltaic System (PV)	1020.63	153.09	15.0	950.41	153.09	16.1
Solar Field (SF)	55.67	33.40	60.0	51.84	31.10	60.0
Solar Receiver (SR)	33.40	28.39	85.0	31.10	13.78	44.3[2]

[1] The wind farm is part of the arrangement (I) WF-SOEC, and the photovoltaic system is part of the arrangement (II) PV-SOEC.
[2] Only physical exergy of the steam was considered for the calculation for the solar receiver.

https://doi.org/10.52202/069564-0018

The results of the analysis conducted for the electrolyzer, heat exchangers, and compressors are presented in Tab. 3. The SOEC exergy efficiency is 89.4%. The losses in the electrolyzer occurs due to overvoltage at the anode and cathode, as well as ohmic resistance of the cells [26]. The thermoneutral voltage (V_{TN}) is 1.288 V, the ohmic heat flux (q''_R) is 0.163 W/cm², and the average power consumed ($\dot{W}_{TN}$) is 17.67 MW, which corresponds to 92.3% of the electricity demanded in the plant.

Table 3. Energy and exergy analysis: SOEC, heat exchangers, and compressors

Components	Energy Analysis			Exergy Analysis		
	Power (kW)	Rejected (kW)	Energy Efficiency (%)	Destroyed (kW)	External Losses (kW)	Exergy[2] Efficiency (%)
Electrolyzer (SOEC)	17671.20	0	100.0	1864.69	0	89.4
Heat Exchanger 1 (HX-1)	-	0	100.0	729.33	0	40.2
Heat Exchanger 2 (HX-2)	-	878.64	-	0	153.45	-
Compressor 1 (CP-1)	483.97	0	100.0	56.17	0	88.4
Heat Exchanger 3 (HX-3)	-	483.70	-	0	131.03	-
Compressor 2 (CP-2)	496.38	0	100.0	57.26	0	88.5
Heat Exchanger 4 (HX-4)	-	505.10	-	0	135.82	-
Heat Exchanger 5 (HX-5)	-	0	100.0	332.23	0	34.9
Heat Exchanger 6 (HX-6)	-	6.54	-	0	0.18	-
Compressor 3 (CP-3)	240.25	0	100.0	28.40	0	88.2
Heat Exchanger 7 (HX-7)	-	241.46	-	0	63.99	-
Compressor 4 (CP-4)	245.28	0	100.0	28.72	0	88.3
Heat Exchanger 8 (HX-8)	-	257.42	-	0	67.50	-
Total	19137.10	2372.86	87.6	3096.80	551.97	80.9

[2] Only physical exergy was considered for the calculation of the heat exchangers.

Heat recovery exchangers HX-1 and HX-5 achieved low exergy efficiencies due to the high mean temperature difference between the fluids. Therefore, one of the enhancements that can be made in this plant involves modifying the configuration of these exchangers or changing the method of heat recovery. In the other exchangers, the heat is rejected to the environment, which represents an exergy rate of 552 kW, enough to feed at least one of the compressors. Despite this, the efficiency of the set of electrolyzer, exchangers and compressors is 80.9%.

The overall energy efficiency for the WF-SOEC configuration is 31.08%, and 15.10% for the PV-SOEC arrangement. The overall exergy efficiency is 26.53% and 13.74%, respectively. The energy losses and exergy destroyed are detailed in the Sankey and Grassmann diagrams in Fig. 7 and 8 for both configurations.

Regarding other studies, Lin and Haussener [14] obtained an energy efficiency of 9.9% for a different PV-SOEC arrangement. Restrepo et al. [17] obtained an efficiency of 31.8% for a PV-SOEC system but used PV panels with solar concentration (CPV) that achieve efficiencies far above conventional PV cells (36.3% versus 15.0%). Nasser and Hassan [19] obtained an efficiency value of 18.6% considering a WF-SOEC plant configuration. However, it is difficult to make direct comparisons among these studies due to variations in plant configuration, modes of operation, and locations considered for the analyses.

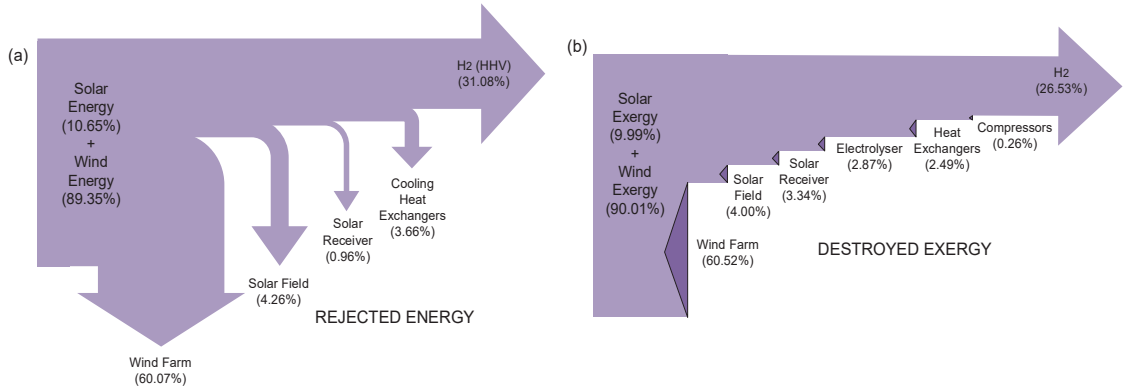

Figure 7. Energy and Exergy Diagrams for the WF-SOEC plant: (a) Sankey and (b) Grassmann

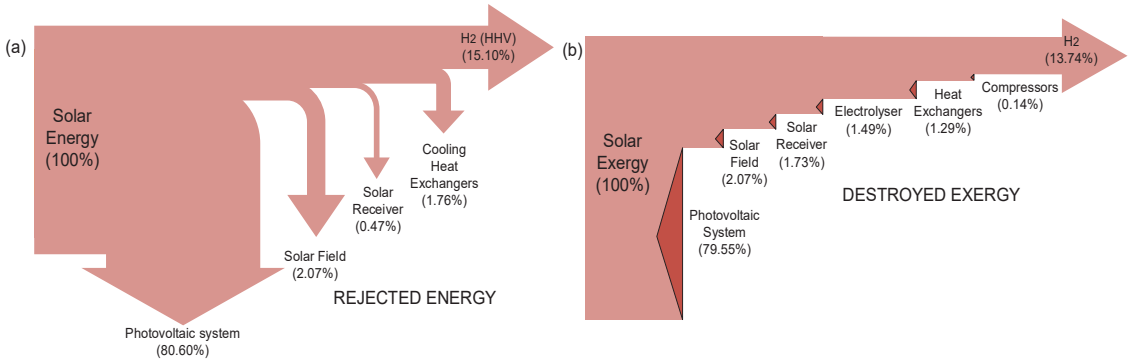

Figure 8. Energy and exergy diagrams for the PV-SOEC plant: (a) Sankey and (b) Grassmann

In the exergoeconomic analysis, the extraction method is adopted in the electrolyzer since hydrogen is considered the main product of the plant. However, as the total exergy of hydrogen at the electrolyzer outlet is almost 30 times higher than the total exergy of oxygen, there will be no significant differences in costs if the equality method is applied.

The unit exergy costs for each stream are presented in Fig. 9a for the WF-SOEC arrangement, where A and B are the exergy fluxes of solar irradiation, C is the flow of wind exergy, and D is the electricity generated by the wind turbines. As the streams A, C, and 1 are the inputs used in the first process of the plant, their exergy costs are considered equal to the unit. The unit exergy costs obtained for solar exergy in the solar receiver, electricity, and steam are 1.67, 3.30, and 4.26 kJ/kJ, respectively. For oxygen, the estimated unit exergy cost is 4.78 kJ/kJ, and for hydrogen at the end of the process, it is 3.89 kJ/kJ.

The unit exergy costs for the PV-SOEC plant are presented in Fig. 9b. As the efficiency of the photovoltaic system is less than half that of the wind system, the exergy costs are significantly higher. The unit cost of electricity is 6.72, steam is 6.35, and for oxygen, it is 9.61 kJ/kJ. For hydrogen, it is 7.53 kJ/kJ, which is 94% higher than in the previous configuration.

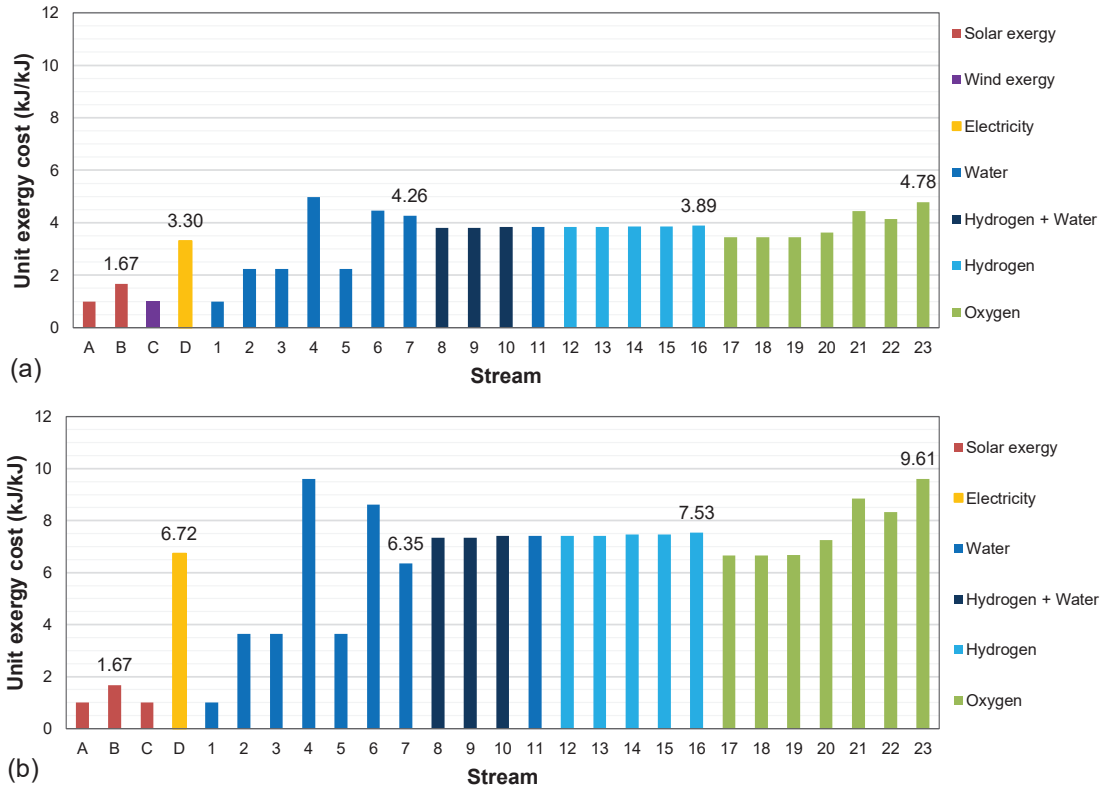

Figure 9. Unit exergy costs: (a) WF-SOEC and (b) PV-SOEC

https://doi.org/10.52202/069564-0018

Finally, Tab. 4 shows the exergy intensity values for the superheated steam used in the electrolysis process and the gases oxygen and hydrogen produced. In the WF-SOEC plant, 471.96 MJ of exergy is necessary to produce 1 kg of hydrogen, while for the PV-SOEC plant, it is 913.69 MJ. Although these values are high compared to the chemical exergy of H_2, in both cases, the exergy used is 100% obtained from renewable resources and without direct CO_2 emissions, which gives a significant advantage compared to the currently predominant production processes in the hydrogen industry. Moreover, these arrangements can be optimized to achieve higher levels of efficiency and lower exergy costs.

Table 4. Exergy Intensity

Plant	Stream	Exergy intensity (MJ/kg)
WF-SOEC	H_2O (850ºC, 1 bar)	8.00
	O_2 (25ºC, 30 bar)	1.84
	H_2 (25ºC, 30 bar)	471.96
PV-SOEC	H_2O (850ºC, 1 bar)	11.91
	O_2 (25ºC, 30 bar)	3.69
	H_2 (25ºC, 30 bar)	913.69

5. Conclusions

This study provides a comprehensive energy, exergy, and exergoeconomic assessment for two hydrogen production plants based on the high-temperature electrolysis (HTE) route. The analyses were carried out for Pecém, a coastal district located in north-eastern Brazil. In the proposed plants, the thermal demand is supplied by solar energy from a solar tower system. For the electrical demand, wind turbines and photovoltaic panels were evaluated.

Assuming the generation of a wind farm with 10 MW of installed capacity as a reference, the daily H_2 production was estimated at 4.13 t. The SOEC exergy efficiency was 89.4%. The overall energy efficiency for the WF-SOEC configuration was 31.08%, and 15.10% for the PV-SOEC arrangement. The overall exergy efficiency was 26.53% and 13.74%, respectively. In the exergoeconomic analysis, the unit exergy cost of hydrogen was 3.89 for the WF-SOEC, and 7.53 for the PV-SOEC configuration.

Regardless the efficiencies and the exergy costs achieved, it is important to note that in both arrangements evaluated, the exergy used is obtained 100% from renewable resources and without direct CO_2 emissions. This gives a significant advantage over the predominant production processes in the hydrogen industry. The SOEC technology, while still undergoing research and development, offers a promising alternative for hydrogen production with the potential for further optimization of efficiency levels and lower exergy costs. Furthermore, this study provides a basis for future investigations into HTE-based hydrogen production plants and serves as a contribution to the transition towards sustainable energy systems.

Acknowledgments

The first author acknowledges Instituto Federal de Educação, Ciência e Tecnologia de Minas Gerais (IFMG) - Campus Formiga for its support during the development of this study. The second author acknowledges CNPq (Conselho Nacional de Desenvolvimento Científico e Tecnológico) for the grant 306484/2020-0.

Nomenclature

A area, m²
b specific exergy, kJ
B exergy, kJ
$\dot{B}$ exergy rate, kW
c unit exergy cost, kJ/kJ
C scale factor
$\dot{C}$ exergy cost rate, kW
$\dot{E}$ energy rate, kW
F Faraday constant, 96,486 C/mol
G Gibbs free energy, kJ
H enthalpy, kJ
i current density, A/cm²
I current, A
j number of electrons
K form factor, m/s
$\dot{Q}$ heat transfer rate, kW
v wind speed, m/s
V voltage, V
W work, kJ
$\dot{W}$ power, kW
$\dot{m}$ mass flow rate, kg/s
q" heat flux, W/cm²

R universal gas constant, 8.314 kJ/(kmol·K)
S entropy, kJ/K
T temperature, °C
y molar fraction

Greek symbols

Δ variation
η efficiency
ρ specific mass, kg/m³
φ exergy intensity, MJ/kg

Subscripts and superscripts

0 standard
inp input
min minimum
N Nerst
O ohmic
$prod$ products
PV photovoltaic system
R reaction
$react$ reactants
SF solar field
TN thermoneutral
WF wind farm

References

[1] F. Dawood, M. Anda, and G. M. Shafiullah, "Hydrogen production for energy: An overview," *Int. J. Hydrogen Energy*, vol. 45, no. 7, pp. 3847–3869, 2020, doi: 10.1016/j.ijhydene.2019.12.059.

[2] E. S. Hanley, J. P. Deane, and B. P. Ó. Gallachóir, "The role of hydrogen in low carbon energy futures–A review of existing perspectives," *Renew. Sustain. Energy Rev.*, vol. 82, no. July, pp. 3027–3045, 2017, doi: 10.1016/j.rser.2017.10.034.

[3] J. Töpler and J. Lehmann, *Hydrogen and Fuel Cells*. New York: Springer, 2016.

[4] IEA, "Net zero by 2050: a roadmap for the global energy sector," International Energy Agency, Paris, 2021. [Online]. Available: https://www.iea.org/reports/net-zero-by-2050

[5] Z. Abdin, A. Zafaranloo, A. Rafiee, W. Mérida, W. Lipiński, and K. R. Khalilpour, "Hydrogen as an energy vector," *Renew. Sustain. Energy Rev.*, vol. 120, no. November 2019, 2020, doi: 10.1016/j.rser.2019.109620.

[6] Hydrogen Council, "Hydrogen for Net-Zero A critical cost-competitive energy vector," Hydrogen Council and McKinsey & Company, Brussels, 2021.

[7] J. O. Abe, A. P. I. Popoola, E. Ajenifuja, and O. M. Popoola, "Hydrogen energy, economy and storage: Review and recommendation," *Int. J. Hydrogen Energy*, vol. 44, no. 29, pp. 15072–15086, 2019, doi: 10.1016/j.ijhydene.2019.04.068.

[8] IEA, "Global Hydrogen Review 2021.," International Energy Agency, Paris, 2021. doi: -.

[9] M. David, C. Ocampo-Martínez, and R. Sánchez-Peña, "Advances in alkaline water electrolyzers: A review," *J. Energy Storage*, vol. 23, no. April, pp. 392–403, 2019, doi: 10.1016/j.est.2019.03.001.

[10] M. Carmo, D. L. Fritz, J. Mergel, and D. Stolten, "A comprehensive review on PEM water electrolysis," *Int. J. Hydrogen Energy*, vol. 38, no. 12, pp. 4901–4934, 2013, doi: 10.1016/j.ijhydene.2013.01.151.

[11] M. A. Laguna-Bercero, "Recent advances in high temperature electrolysis using solid oxide fuel cells: A review," *J. Power Sources*, vol. 203, pp. 4–16, 2012, doi: 10.1016/j.jpowsour.2011.12.019.

[12] J. E. O'Brien, "Thermodynamics and transport phenomena in high temperature steam electrolysis cells," *J. Heat Transfer*, vol. 134, no. 3, pp. 1–11, 2012, doi: 10.1115/1.4005132.

[13] A. Hauch *et al.*, "Recent advances in solid oxide cell technology for electrolysis," *Science (80-.).*, vol. 370, no. 6513, 2020, doi: 10.1126/science.aba6118.

[14] M. Lin and S. Haussener, "Techno-economic modeling and optimization of solar-driven high-temperature electrolysis systems," *Sol. Energy*, vol. 155, pp. 1389–1402, 2017, doi: 10.1016/j.solener.2017.07.077.

[15] D. Yadav and R. Banerjee, "Economic assessment of hydrogen production from solar driven high-temperature steam electrolysis process," *J. Clean. Prod.*, vol. 183, pp. 1131–1155, 2018, doi: 10.1016/j.jclepro.2018.01.074.

[16] L. Mastropasqua, I. Pecenati, A. Giostri, and S. Campanari, "Solar hydrogen production: Techno-economic analysis of a parabolic dish-supported high-temperature electrolysis system," *Appl. Energy*, vol. 261, no. December 2019, p. 114392, 2020, doi: 10.1016/j.apenergy.2019.114392.

[17] J. C. Restrepo, D. Luis Izidoro, A. Milena Lozano Násner, O. José Venturini, and E. Eduardo Silva Lora, "Techno-economical evaluation of renewable hydrogen production through concentrated solar energy," *Energy Convers. Manag.*, vol. 258, p. 115372, Apr. 2022, doi: 10.1016/j.enconman.2022.115372.

[18] M. Mohebali Nejadian, P. Ahmadi, and E. Houshfar, "Comparative optimization study of three novel integrated hydrogen production systems with SOEC, PEM, and alkaline electrolyzer," *Fuel*, vol. 336, no. November 2022, p. 126835, 2023, doi: 10.1016/j.fuel.2022.126835.

https://doi.org/10.52202/069564-0018

[19] M. Nasser and H. Hassan, “Techno-enviro-economic analysis of hydrogen production via low and high temperature electrolyzers powered by PV/Wind turbines/Waste heat,” *Energy Convers. Manag.*, vol. 278, no. November 2022, p. 116693, 2023, doi: 10.1016/j.enconman.2023.116693.

[20] T. J. Kotas, *The exergy method of thermal plant analysis*, no. 1. London: Butterworths, 1985. doi: 10.1016/0378-3804(88)90147-7.

[21] J. Szargut, *Exergy method: technical and ecological applications*, vol. 18. Southampton, UK: WIT Press, 2005.

[22] S. Oliveira Jr., *Exergy: Production, cost and renewability*. London: Springer, 2013. doi: 10.1007/978-1-4471-4165-5.

[23] Z. Li, H. Zhang, H. Xu, and J. Xuan, “Advancing the multiscale understanding on solid oxide electrolysis cells via modelling approaches: A review,” *Renew. Sustain. Energy Rev.*, vol. 141, no. February, p. 110863, 2021, doi: 10.1016/j.rser.2021.110863.

[24] F. Petipas, A. Brisse, and C. Bouallou, “Model-based behaviour of a high temperature electrolyser system operated at various loads,” *J. Power Sources*, vol. 239, no. 2013, pp. 584–595, 2013, doi: 10.1016/j.jpowsour.2013.03.027.

[25] J. B. Hansen, “Solid oxide electrolysis - a key enabling technology for sustainable energy scenarios,” *Faraday Discuss.*, vol. 182, pp. 9–48, 2015, doi: 10.1039/c5fd90071a.

[26] J. E. O’Brien, “Thermodynamic considerations for thermal water splitting processes and high temperature electrolysis,” *ASME Int. Mech. Eng. Congr. Expo. Proc.*, vol. 8, pp. 639–651, 2009, doi: 10.1115/IMECE2008-68880.

[27] D. G. Goodwin, H. K. Moffat, I. Schoegl, R. L. Speth, and B. W. Weber, “Cantera: An object-oriented software toolkit for chemical kinetics, thermodynamics, and transport processes.” 2022. doi: 10.5281/zenodo.6387882.

[28] I. H. Bell, J. Wronski, S. Quoilin, and V. Lemort, “Pure and pseudo-pure fluid thermophysical property evaluation and the open-source thermophysical property library coolprop,” *Ind. Eng. Chem. Res.*, vol. 53, no. 6, pp. 2498–2508, 2014, doi: 10.1021/ie4033999.

[29] D. Izidoro and S. Oliveira Jr., “Energy and Exergy Analysis of Hydrogen Production Via High-Temperature Electrolysis Powered By Solar and Wind Energy,” 2021. doi: 10.26678/abcm.cobem2021.cob2021-0368.

[30] M. Lin and S. Haussener, “Techno-economic modeling and optimization of solar-driven high-temperature electrolysis systems,” *Sol. Energy*, vol. 155, pp. 1389–1402, 2017, doi: 10.1016/j.solener.2017.07.077.

[31] Vestas, “2 MW platform - V100,” 2023. https://www.vestas.com/en/products/2-mw-platform/V100-2-0-MW

[32] C. Xu, Z. Wang, X. Li, and F. Sun, “Energy and exergy analysis of solar power tower plants,” *Appl. Therm. Eng.*, vol. 31, no. 17–18, pp. 3904–3913, 2011, doi: 10.1016/j.applthermaleng.2011.07.038.

[33] Governo do Ceará, “Complexo Portuário do Pecém: Hub de Hidrogênio Verde,” 2023. https://www.complexodopecem.com.br/hubh2v/

[34] M. Sengupta, Y. Xie, A. Lopez, A. Habte, G. Maclaurin, and J. Shelby, “The National Solar Radiation Data Base (NSRDB),” *Renew. Sustain. Energy Rev.*, vol. 89, no. March, pp. 51–60, 2018, doi: 10.1016/j.rser.2018.03.003.

[35] NREL, “National Solar Radiation Database (NSRDB),” 2022. nsrdb.nrel.gov/ (accessed Jan. 13, 2022).

[36] CEPEL, “Atlas do Potencial Eólico Brasileiro: Simulações 2013,” Centro de Pesquisas de Energia Elétrica, Rio de Janeiro, 2017.

[37] M. O. Pinto, "Wind Energy Fundamentals", 1st ed. Rio de Janeiro: LTC, 2018.

[38] K. Christopher and R. Dimitrios, “A review on exergy comparison of hydrogen production methods from renewable energy sources,” *Energy Environ. Sci.*, vol. 5, no. 5, pp. 6640–6651, 2012, doi: 10.1039/c2ee01098d.

[39] R. Petela, *Engineering Thermodynamics of Thermal Radioation For Solar Power Utilization*. New York: McGraw Hill, 2010.

[40] R. A. Gaggioli and W. J. Wepfer, “Exergy economics: I. Cost accounting applications,” *Energy*, vol. 5, no. 8–9, pp. 823–837, 1980, doi: 10.1016/0360-5442(80)90099-7.

[41] J. A. M. Silva, “Exergo-environmental performance of oil processing and its derivatives,” Department of Mechanical Engineering" Departament of Mechanical Engineering, Escola Politécnica, Universidade de São Paulo. São Paulo, PhD Thesis, 2013.